Translesional Synthesis on a DNA Template Containing a Single Stereoisomer of dG-(+)- or dG-(−)-*anti*-BPDE (7,8-Dihydroxy-*anti*-9,10-epoxy-7,8,9,10-tetrahydrobenzo[*a*]pyrene)†

Shinya Shibutani,*,‡ Leonid A. Margulis,§ Nicholas E. Geacintov,§ and Arthur P. Grollman‡

Department of Pharmacological Sciences, State University of New York at Stony Brook, Stony Brook, New York 11794-8651, and Department of Chemistry, New York University, New York, New York 10003

Received December 11, 1992; Revised Manuscript Received April 15, 1993

ABSTRACT: Oligodeoxynucleotides modified site-specificially with dG-(+)-*trans*- and dG-(+)-*cis*-*anti*-BPDE (7,8-dihydroxy-9,10-epoxy-7,8,9,10-tetrahydrobenzo[*a*]pyrene) or dG-(−)-*trans*- and dG-(−)-*cis*-*anti*-BPDE were used as templates in primer extension reactions catalyzed by the Klenow fragment of *Escherichia coli* DNA polymerase I. The primer could be extended past the dG-(−)-*trans*-BPDE adduct with small amounts of dAMP incorporated opposite the lesion. A small amount of base deletions was also observed while, with the dG-(−)-*cis*-BPDE adduct, one- and two-base deletions predominated. When templates containing dG-(+)-*trans*-BPDE were used, small amounts of products containing one-base deletions were observed; with dG-(+)-*cis*-BPDE, substitution of dAMP opposite the lesion was also detected. The frequency of nucleotide insertion for dAMP opposite dG-(−)-*trans*-BPDE and the frequency of extension from the primer terminus containing the dA:dG-(−)-*trans*-BPDE pair were much higher than those observed with the other, stereochemically different BPDE adducts. Kinetic studies were in agreement with the results of the primer extension study. When the base flanking the 5′ side of dG-BPDE was changed from dC to dT, the frequency of one-base deletions increased. We conclude that the *trans*- or *cis*-addition product of dG-(−)-*anti*-BPDE has a higher miscoding potential than dG-(+)-*anti*-BPDE in our model system and that G→T transversions and deletions predominate. These observations are consistent with the types of mutations observed *in vivo*.

The environmental carcinogen benzo[*a*]pyrene (BP) is metabolized by hepatic cytochrome P-450 and epoxide hydratase to form (−)-BP 7,8-dihydrodiol and (+)-BP 7,8-dihydrodiol (Yang *et al.*, 1976; Yang & Gelboin, 1976). (−)-BP 7,8-dihydrodiol is carcinogenic to newborn mice, whereas its enantiomer, (+)-BP 7,8-dihydrodiol, has little or no activity (Kapitulnik *et al.*, 1978). (−)-BP 7,8-dihydrodiol can be metabolized to (−)-*syn*- and (+)-*anti*-BPDE,[1] while (+)-BP 7,8-dihydrodiol is converted to (+)-*syn*- and (−)-*anti*-BPDE (Yang *et al.*, 1976; Yang & Gelboin, 1976; Kapitulnik et al., 1978; Thakker *et al.*, 1976, 1977a).

Racemic *anti*-BPDE is reported to be more mutagenic than the diastereomer (±)-*syn*-BPDE (Newbold & Brookes, 1976; Newbold *et al.*, 1979; Huberman *et al.*, 1976; Malavelle *et al.*, 1977; Hsu *et al.*, 1979). Each diastereomer can be resolved into two enantiomers, and striking differences in the biological activities of the (+)- and (−)-enantiomers of *anti*-BPDE (Figure 1) have been reported. The (+)-*anti*-BPDE isomer is tumorigenic on mouse skin (Slaga *et al.*, 1979) and in the lungs of newborn mice (Buening *et al.*, 1978), while the (−)-*anti*-BPDE enantiomer is not. The mutagenic efficiencies of the two enantiomers are different in selected bacterial and mammalian cell systems: in *Salmonella typhimurium* cells (strain T98), the mutagenic activites of the (+)- and (−)-enantiomers are almost equal, but in the TA100 strain (Wood *et al.*, 1977), as well as in mammalian Chinese hamster ovary cells (V79 cells), the activity of the (+)-isomer is 4–6 times greater than that of (−)-*anti*-BPDE (Wood *et al.*, 1977; Brookes & Osborne 1982). However, Burgess *et al.* (1985) reported that the mutagenic efficiency (mutation frequency per DNA lesion) of (−)-*anti*-BPDE was higher than that of the (+)-enantiomer at two separate gene loci in *S. typh-*

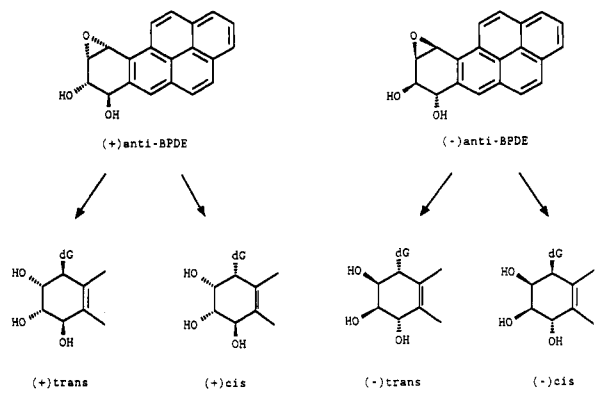

FIGURE 1: Structures of dG-N2-BPDE stereoisomers.

† Work conducted at New York University was supported by the Office of Health and Environmental Research, the Department of Energy (Grant DE-FGO2-86ER60405), and, in part, by Grant CA 20851 from the U.S. Public Health Service, Department of Health and Human Services, awarded by the National Cancer Institute. Studies at Stony Brook were supported by Grants ES04068 from NIEHS and CA17395 from NCI.

‡ State University of New York at Stony Brook.

§ New York University.

[1] Abbreviations used: BPDE, 7,8-dihydroxy-9,10-epoxy-7,8,9,10-tetrahydrobenzo[*a*]pyrene; (+)-*anti*-BPDE, (+)-7β,8α-dihydroxy-9α,-10α-epoxy-7,8,9,10-tetrahydrobenzo[*a*]pyrene(7*R*,8*S*,9*S*,10*R* steric configuration); (−)-*anti*-BPDE, (−)-7α,8β-dihydroxy-9β,10β-epoxy-7,8,9,10-tetrahydrobenzo[*a*]pyrene (7*S*,8*R*,9*R*,10*S* steric configuration); (+)-*syn*-BPDE, (+)-7α,8β-dihydroxy-9α,10α-epoxy-7,8,9,10-tetrahydrobenzo[*a*]pyrene; (−)-syn-BPDE, (−)-7β,8α-dihydroxy-9β,10β-epoxy-7,8,9,10-tetrahydrobenzo[*a*]pyrene; dG, 2′-deoxyguanosine; dNTP, 2′-deoxynucleotide triphosphate; pol I, DNA polymerase I; exo⁻, 3′→5′ exonuclease-free Klenow fragment; exo⁺, intact Klenow fragment; K_M, Michaelis constant; V_{max}, the maximum rate of the reaction; F_{ins}, frequency of insertion; F_{ext}, frequency of extension; PAGE, polyacrylamide gel electrophoresis; HPLC, high-performance liquid chromatography; RT, retention time; Δ, deletion.

0006-2960/93/0432-7531$04.00/0

imurium TA100. Although the same adduct distributions are found in both the bacterial and the human cells, the relative mutagenicity of (+)-*anti*-BPDE is about 7 times higher (per DNA adduct) than that of the (−)-enantiomer in diploid human fibroblasts, while in *S. typhimurium* TA100 the (−)-enantiomer is 4 times more mutagenic than (+)-*anti*-BPDE (Stevens *et al.*, 1985). It was concluded that the BPDE–DNA adduct conformation is important in determining whether a mutation will result. The differences in mutagenicities show that the same lesions are processed differently in human and bacterial cells.

Both (+)- and (−)-*anti*-BPDE react chemically with native DNA to form covalent adducts. Both stereoisomers, especially (+)-*anti*-BPDE, bind by *trans*- and *cis*-addition of N2-guanine (Figure 1) at the C10 position of BPDE (Weinstein *et al.*, 1976; Osborne *et al.*, 1978, 1981; Jeffrey *et al.*, 1976; Koreeda *et al.*, 1978). A smaller fraction of N6-adenine adducts are also formed (Jeffrey *et al.*, 1979; Meehan & Straub, 1979), especially in the case of (−)-*anti*-BPDE (Brookes & Osborne, 1982; Cheng *et al.*, 1989). The formation of unstable N7 adducts has also been reported (Osborne *et al.*, 1978, 1981; King *et al.*, 1979). Most of the previous studies of mutation spectra in bacterial and mammalian cells were performed with racemic *anti*-BPDE (Mizusawa *et al.*, 1981; Eisenstadt *et al.*, 1982; Chakrabarti *et al.*, 1984; Vousden *et al.*, 1986; Yang *et al.*, 1987, 1991; Roilides *et al.*, 1988; Mazur & Glickman, 1988; Chen *et al.*, 1990, 1991; Carothers *et al.*, 1990; Bernelot-Moens *et al.*, 1990; Keohavong & Thilly, 1992). It is not clear from these studies which of the several different adducts are correlated with the mutations observed. Two studies have been published recently in which the optically pure (+)-*anti*-BPDE enantiomer was used (Wei *et al.*, 1991; Rodriguez & Loechler, 1993). While the heterogeneity of adducts in these studies is significantly reduced in this way, it is still not possible to differentiate between effects due to isomeric adducts produced by *cis*- and *trans*-addition. The site-directed mutagenesis experiments of Mackay *et al.* (1992), which are based on a unique (+)-*anti*-BPDE–N2-guanine lesion, constitute an important first step toward resolving these issues.

Oligodeoxynucleotides containing stereospecific and site-specifically-placed lesions are useful in answering these questions (Basu & Essigmann, 1988). Benasutti *et al.* (1988) reacted oligodeoxynucleotides with (+)-*anti*-BPDE; however, the yield of reaction products was quite low. Cosman *et al.* (1990) prepared oligodeoxynucleotides containing single *trans*- and *cis*-addition products of (+)-*anti*- and (−)-*anti*-BPDE covalently bound to the exocyclic amino group of dG (*cis* and *trans* stereochemistry is defined in Figure 1). The availability of modified oligonucleotides offers the possibility of correlating chemical and stereochemical adduct structure with mutation spectra. Site-directed mutagenesis experiments can be useful in this respect (Singer & Essigman, 1991). The inhibition of DNA polymerases (Larson & Strauss, 1987; Brown & Romano, 1991; Thrall *et al.*, 1992) and *trans* lesion synthesis past polycyclic aromatic hydrocarbon–oligonucleotide adducts has been recently described (Reardon *et al.*, 1990; Hruszkewycz & Dipple, 1991; Hruszkewycz *et al.*, 1991). We have developed a novel *in vitro* system that allows us to quantify the frequencies of base substitutions and deletions opposite damaged adducts in reactions involving a primed DNA template containing a defined adduct and various DNA polymerases (Shibutani *et al.*, 1991a).

In the present paper, we explore the miscoding properties of stereoisomers of dG-(+)- and dG-(−)-*anti*-BPDE and determine the kinetic parameters of reactions in which dNTPs are inserted opposite the adduct (F_{ins}) and extended from the 3′ primer terminus (F_{ext}). Our results indicate that *cis*- and *trans*-addition products of dG-(−)-*anti*-BPDE adducts have a higher miscoding potential than those formed from dG-(+)-*anti*-BPDE and predict that these adducts, if unrepaired, can lead *in vivo* to targeted G→T transversions and deletions at the site of the lesion.

EXPERIMENTAL PROCEDURES

Materials. Organic chemicals used for the synthesis of oligodeoxynucleotides were supplied by Aldrich Chemical. Acetonitrile, triethylamine, and distilled water, all HPLC grade, were purchased from Fisher Chemical. [γ-^{32}P]ATP (specific activity, >5000 Ci/mmol) was obtained from Amersham Corp. Cloned exo$^-$ (21 200 units/mg) and exo$^+$ Klenow fragments of *Escherichia coli* polymerase I were purchased from United State Biochemical Corp.; intact DNA pol I and deoxynucleotide triphosphate from Pharmacia; T4 polynucleotide kinase from Stratagene; and venom phosphodiesterase I from Sigma. A Waters 990 HPLC instrument, equipped with a photodiode array detector, was used for separation and analysis of modified and unmodified oligodeoxynucleotides. The diol epoxides (+)- and (−)-*anti*-BPDE were obtained from the National Cancer Institute Chemical Carcinogen Reference Standard Repository.

Synthesis and Modification of Oligodeoxynucleotides. Oligodeoxynucleotides were prepared using solid-state synthesis on an automated DNA synthesizer (Takeshita *et al.*, 1987). The 18-mers, 5′-CCTTCXCTCCTTTCCTCT (X = modified position), containing single dG-(+)-*trans*-BPDE, dG-(−)-*trans*-BPDE, dG-(+)-*cis*-BPDE, or dG-(−)-*cis*-BPDE lesions, were prepared, isolated, and purified according to procedures previously outlined (Cosman *et al.*, 1990; Geacintov *et al.*, 1991). Briefly, a 60 μM solution of 18-mer (concentration of single strands) in 20 mM sodium phosphate buffer and 1.7% triethylamine (Geacintov *et al.*, 1991) was incubated with either stereoisomer of *anti*-BPDE (molar ratio [BPDE]/[DNA strands] = 0.7) for 3 h; using the same solution, this procedure was repeated 2 more times so that the overall dose of [BPDE]/[DNA strand] was ≈2:1. The modified oligonucleotides were separated from unmodified DNA strands by reverse-phase HPLC. Stereochemical characteristics of the adducts were established by enzyme digestion to the nucleoside and BPDE–nucleoside adduct levels, and comparisons were made of their circular dichroism spectra and reverse-phase HPLC elution times with those of dG-N^2-BPDE standards (Cheng *et al.*, 1989), as described previously in detail (Cosman *et al.*, 1990; Geacintov *et al.*, 1991).

Finally, the separated modified and unmodified oligodeoxynucleotides were repurified by HPLC, followed by PAGE, followed again by HPLC. Electrophoresis was on 20% polyacrylamide gel containing 7 M urea (15 × 72 × 0.04 cm). In HPLC experiments, a reverse-phase μBondapak C_{18} column (0.39 × 30 cm^2, Waters) was employed using a linear gradient of 0.05 M triethylamine acetate, pH 7.0, containing 10–20% acetonitrile, an elution time of 60 min, and a flow rate of 1.0 mL/min, as described elsewhere (Shibutani *et al.*, 1991b).

Unmodified and BPDE-modified 18-mers (5 pmol) were labeled with ^{32}P at the 5′ terminus using T4 polynucleotide kinase and [γ-^{32}P]ATP and then subjected to 20% polyacrylamide gel electrophoresis in the presence of 7 M urea to check for impurities.

Primer Extension Reaction. As described previously (Shibutani *et al.*, 1991a), the 18-mer template containing a single dG or BPDE-modified dG was annealed with a ^{32}P-

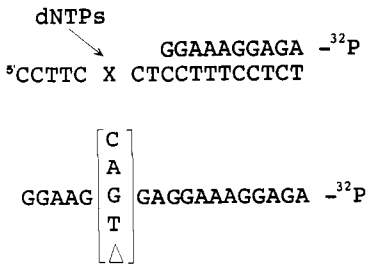

FIGURE 2: Schematic diagram of the primer extension method. (a) Insertion of dNTP opposite the modified dG (X). (b) Possible base sequences of a fully extended primer (Δ = deleted base).

labeled 10-mer primer (5'-AGAGGAAAGG). Primer extension was carried out in 10 μL of buffered solution containing the Klenow fragment of *E. coli* DNA polymerase I, four dNTPs (100 μM each), and the unmodified or dG-BPDE-modified template primed with the ^{32}P-labeled 10-mer, as shown in Figure 2. The Klenow fragment containing (exo$^+$) or lacking (exo$^-$) 3'→5' exonuclease activity was incubated at 25 °C for 1 h in 50 mM Tris-HCl buffer (pH 8.0) containing 8 mM $MgCl_2$ and 5 mM 2-mercaptoethanol. Reaction mixtures were subjected to 20% PAGE (15 × 72 × 0.04 cm) in the presence of 7 M urea. Following electrophoresis, positions of the oligomers were established by autoradiography, using Kodak X-Omat XAR film. Standards representing a 17-mer containing a single deletion or 18-mer containing dA, dC, dG, or dT at position 13 were prepared by solid-state synthesis (Takeshita *et al.*, 1987). Standards labeled with ^{32}P (0.1 pmol) were partially digested at 25 °C for 2 min with venom phosphodiesterase I (1.0×10^{-5} units, Sigma) in 10 μL of 100 mM Tris-HCl buffer (pH 8.0) for comparison with incompletely extended primers.

Kinetic Studies. The kinetic parameters of base insertion and chain extension were determined under conditions similar to those reported previously (Shibutani *et al.*, 1991a). Reaction mixtures containing 0.0005–0.05 units of exo$^-$ Klenow fragment were incubated at 30 °C for 90 s to 6 min in 10 μL of Tris-HCl buffer (pH 8.0) containing template DNA (5'-CCTTCXCTCCTTTCCTCT, X = dG or dG-BPDE) primed with ^{32}P-labeled 12-mer (5'-AGAGGAAAGGAG) for insertion kinetics or with a ^{32}P-labeled 13-mer containing dC, dA, dG, or dT (5'-AGAGGAAAGGAGN, N = C, A, G, or T) to measure chain extension.

Base insertion was measured in reactions using 0.0005 units of polymerase for 90 s (C:G); 0.01 units for 90 s (T:G); 0.025 units for 90 s (A:G, G:G); 0.05 units for 90 s (A:G (–)-*trans* and G:G (–)-*trans*); and 0.05 units for 6 min for other pairs. Kinetics of extension were measured in reactions using 0.0005 units of enzyme for 90 s (C:G); 0.001 units for 90 s (T:G); 0.05 units for 90 s (G:G); and 0.05 units for 6 min for other pairs. Samples were heated for 3 min at 95 °C in the presence of formamide dye and then applied to 20% PAGE (35 × 42 × 0.04 cm^3) in the presence of urea. Bands were identified by autoradiography and excised from the gel, and the radioactivity of the sample was determined. Radioactivity was measured in a Packard scintillation counter using Liquiscint (National Diagnostics). The Michaelis constant (K_M) and maximum rate of reaction (V_{max}) were obtained from Hanes–Woolf plots. Data represent an average of 2–4 independent experiments. Frequencies of base insertion (F_{ins}) and chain extension (F_{ext}) were determined relative to dC:dG according to equations derived by Mendelman *et al.* (1989, 1990), where $F = (V_{max}/K_m)$[wrong pair]$/(V_{max}/K_m)$[right pair = dC:dG], with "wrong pair" defined as a mismatch or any pair involving BPDE-modified dG.

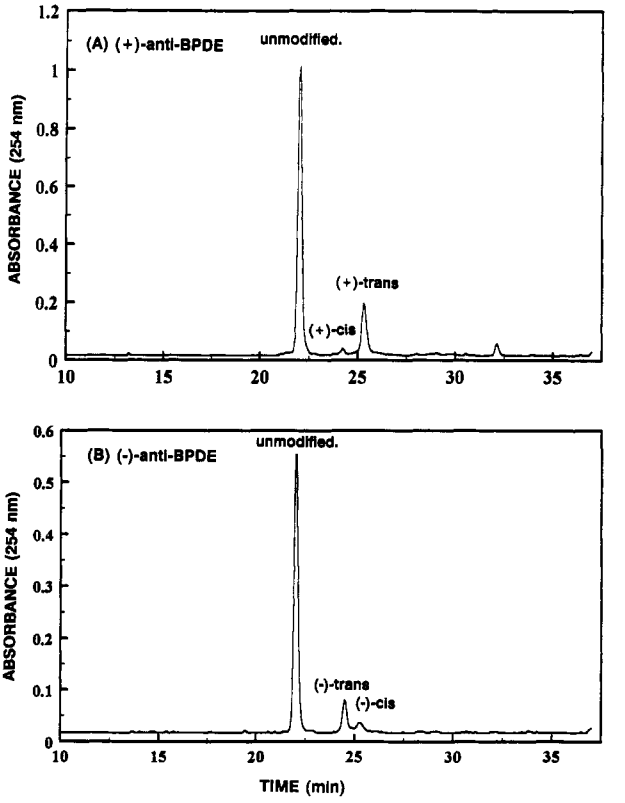

FIGURE 3: HPLC elution profiles of reaction mixtures of the oligonucleotide d(CCTTCGCTCCTTTCCTCT) with (A) (+)-*anti*-BPDE and (B) (–)-*anti*-BPDE (0–90% methanol/20 mM sodium phosphate buffer gradient, pH 7.0, 60 min, flow rate 3.0 mL/min).

RESULTS

BPDE–Oligonucleotide Adducts. Typical HPLC elution profiles of (+)-*anti*-BPDE- and (–)-*anti*-BPDE–oligonucleotide reaction mixtures are shown in Figures 3A and 3B, respectively (semipreparative 9.4 × 250 mm 5 μm Shandon ODS-Hypersil column, purchased from Keystone Scientific, Bellefonte, PA). In Figure 3A, the peaks eluting at 22.0, 24.2, and 25.3 min represent unmodified, (+)-*cis*-BPDE-, and (+)-*trans*-BPDE-modified oligonucleotides, respectively. The (–)-*trans*-BPDE- and (–)-*cis*-BPDE-modified 18-mers elute at 24.5 and 25.3 min, respectively (Figure 3B; due to partial overlap between these two eluates, each fraction was collected and subjected to a second HPLC reverse-phase purification step employing a 0–45% MeOH/aqueous buffer gradient (1 h, 3.0 mL/min, data not shown). The absorption spectra of the modified oligonucleotides were similar to one another and to those published earlier using another sequence (Cosman *et al.*, 1990), with maxima at 350 nm attributable to the pyrenyl residue.

CD spectra of the four stereochemically different *anti*-BPDE–oligonucleotide adducts (Figure 4) resemble those obtained for another BPDE-modified oligonucleotide sequence (Geacintov *et al.*, 1991). A prominent induced CD spectrum is evident in the 300–360-nm region of the spectrum of both *trans*-adducts (Figure 4A) but not in the case of the *cis*-adducts (Figure 4B). Induced CD spectra are due to the pyrenyl moieties in the different lesions; therefore, differences in magnitudes of induced CD signals must reflect differences in the microenvironments of the aromatic BPDE residues with *trans* and *cis* stereochemistry in these flexible, single-stranded oligonucleotides, the precise nature of which cannot be specified on the basis of these spectra.

HPLC elution profiles of the enzyme-digested unmodified 18-mer and the (+)-*trans*-BPDE-modified 18-mer are shown

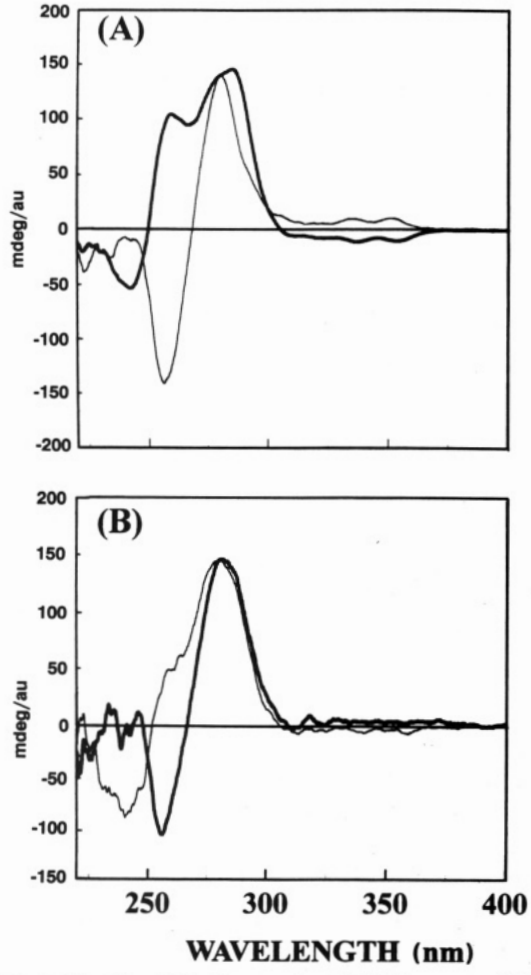

FIGURE 4: Circular dichroism spectra of (A) *trans*- and (B) *cis*-BPDE-N2-dG–oligonucleotide adducts (18-mers). Heavy lines: adducts derived from reaction with (+)-*anti*-BPDE. Thin lines: adducts derived from reaction with (–)-*anti*-BPDE. The vertical axes (±15% accuracy) are expressed in units of mdeg/(absorbance unit at 350 nm); the ellipticity is expressed per absorbance unit (au) at an arbitrary wavelength in the absorption spectrum of the modified oligonucleotides rather than per mole of adducted oligonucleotide because of uncertainties in the molar extinction coefficients of the adducted pyrenyl chromophores (Cheng *et al.*, 1989; Weems & Yang, 1989).

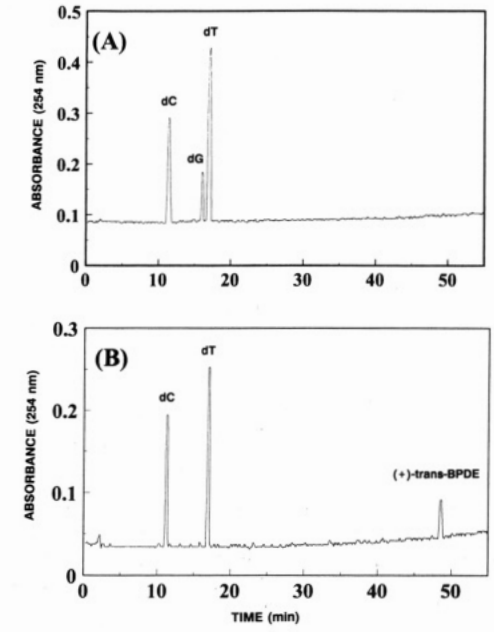

FIGURE 5: HPLC elution profiles of enzyme digests of (A) unmodified 18-mer oligonucleotide and (B) the (+)-*trans*-dG–oligonucleotide adduct (modified and unmodified oligonucleotides were digested to nucleosides with snake venom phosphodiesterase and bacterial alkaline phosphatase, according to the procedure of Cosman *et al.*, 1990).

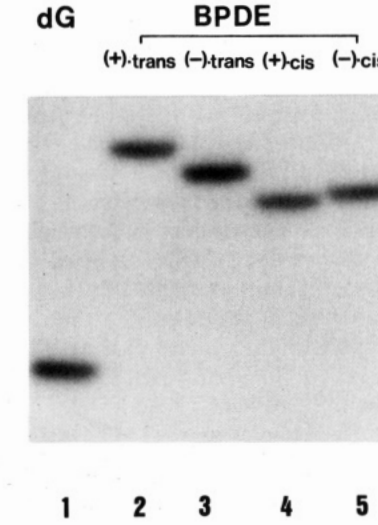

FIGURE 6: Polyacrylamide gel electrophoresis of 18-mers containing a single isomeric dG-N2-BPDE adduct. Oligodeoxynucleotides were labeled with ^{32}P as described in Experimental Procedures and then subjected to electrophoresis on 20% polyacrylamide (15 × 75 × 0.04 cm); lane 1, unmodified template strand, and lanes 2–5, modified template strands.

in Figures 5A and 5B, respectively (0–90% MeOH/aqueous buffer gradient, 60 min, 1.5 mL/min flow rate, 4.5 × 250 mm analytical column). In Figure 5A, the elution peaks at 11.4, 16.1, and 17.1 min are due to dC, dG, and dT, respectively; on the basis of the relative areas under each peak and the molar extinction coefficients of the bases (data not shown), the relative ratio of dT:dG:dC is 8.5:1.0:8.0, which, within experimental error, agrees with the expected ratio of 9:1:8. In Figure 5B, there is no peak corresponding to the unmodified dG at 16.1 min; however, a peak that coelutes with a standard (+)-*trans*-BPDE-N2-dG–mononucleoside adduct and has the same CD spectrum (data not shown) appears at 48.6 min. Analogous results following enzyme digestion were obtained with the other three stereochemically different adducts, as described in an earlier publication (Geacintov *et al.*, 1991).

Gel Electrophoresis. The purities of 18-mers containing the isomeric dG-BPDE adducts were analyzed on 20% polyacrylamide gel after the 18-mers were labeled with ^{32}P at the 5′ terminus (Figure 6). Electrophoretic migrations of BPDE-modified oligomers (lanes 2–5) were slower than that of unmodified 18-mer (lane 1). Migrations of the (+)-*trans*-BPDE- and (–)-*trans*-BPDE-modified oligomers were slower than those of (+)-*cis*-BPDE- and (–)-*cis*-BPDE-modified oligomers, respectively. All modified oligodeoxynucleotides were purified to homogeneity by HPLC and gel electrophoresis. These results (Figure 6) demonstrate no discernable contamination of the *trans*-modified oligomer by *cis*-modified oligomer and vice versa, following purification of 18-mers modified with (+)-*anti*-BPDE or (–)-*anti*-BPDE. No other bands were observed, even when the gels were exposed for longer periods of time. The limit of detection of contaminating species in these analysis was 0.02%.

Quantitation of Base Substitution and Deletions

Standard Markers. Oligodeoxynucleotides containing dA, dC, dG, dT, or a one-base deletion at position 13 can be distinguished by polyacrylamide gel electrophoresis (Figure

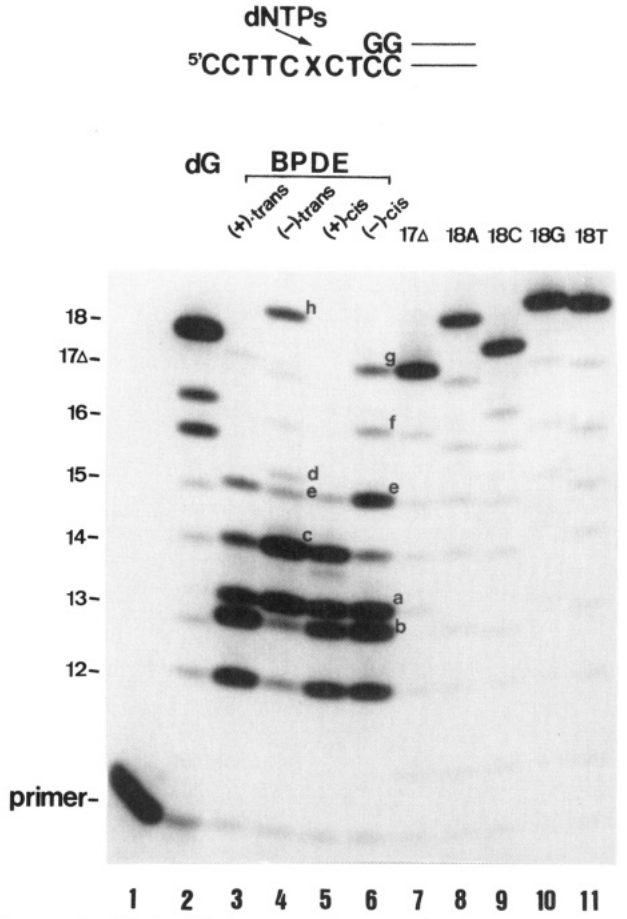

FIGURE 7: Nucleotide incorporation opposite isomeric dG-N2-BPDE–oligonucleotide adducts. Using a 18-mer template containing a single dG or isomeric dG-N2-BPDEs (5′-CCTTCXCTCCTTT-CCTCT, X = dG or dG-N2-BPDEs) primed with ^{32}P-labeled 10-mer, primer extension reactions were conducted at 25 °C for 1 h using 0.005 units of exo$^-$ Klenow fragment for the unmodified 18-mer (lane 2) and 5 units of exo$^-$ Klenow fragment for the modified 18-mers (lanes 3–6), as described under Experimental Procedures. One-third of the reaction mixture was subjected to 20% polyacrylamide gel electrophoresis (15 × 75 × 0.04 cm). Mobilities of the reaction products were compared with 17-mer standards containing a single deletion (lane 7) or an 18-mer containing dA (lane 8), dC (lane 9), dG (lane 10), or dT (lane 11) at position 13, which was partially digested by venom phosphodiesterase I.

7, lanes 7–11). When a mixture of these standards was subjected to gel electrophoresis, the 18-mer containing dA could be distinguished from 18-mers containing dC, dG, and dT (data not shown). These standards were partially digested by venom phosphodiesterase to produce a ladder that could be compared with the migration of the incompletely extended reaction products. DNA synthesis on the unmodified template (lane 2) led to the expected incorporation of dCMP opposite dG at position 13 using 0.005 unit of exo$^-$ Klenow fragment of DNA pol I. Bands representing an incompletely extended 16-mer and 17-mer are present. When the amount of the enzyme was increased to 0.01 units, >98% of the product was fully extended.

BPDE–Oligonucleotide Adducts. Using templates modified with isomeric dG-BPDE at position 13, primer extension by exo$^-$ Klenow fragment was blocked partially either one base before the lesion (position 12) at the base flanking the modified dG on the 5′ side or opposite the lesion. In Figure 7, bands b and c located at position 13 (lanes 3–6) reflect incorporation of dAMP (lower band) and dGMP (upper band) opposite the lesion. In the case of the dG-(−)-*trans*-BPDE adduct (lane 4), a full-length 18-mer containing dA opposite

Table I: Time Course of Primer Extension in Reactions Catalyzed by exo$^-$ Klenow Fragment on Templates Containing Stereoisomers of dG-(+)-*anti*-BPDE or dG-(−)-*anti*-BPDE[a]

lesion	time (min)	dA (%)	Δ^1 (%)	Δ^2 (%)
(+)-*trans*-BPDE				
	10	n.d.	0.06 ± 0.01	n.d.
	30	0.05 ± 0.01	0.19 ± 0.01	0.09 ± 0.01
	60	0.07 ± 0.02	0.53 ± 0.04	0.16 ± 0.06
	120	0.19 ± 0.02	1.66 ± 0.07	0.49 ± 0.06
(−)-*trans*-BPDE				
	10	0.15 ± 0.05	0.11 ± 0.02	0.14 ± 0.06
	30	0.97 ± 0.10	0.28 ± 0.08	0.45 ± 0.03
	60	3.18 ± 0.09	0.58 ± 0.16	0.69 ± 0.12
(+)-*cis*-BPDE	120	9.12 + 0.05	1.43 + 0.03	0.97 + 0.07
	10	n.d.	n.d.	n.d.
	30	0.07 ± 0.02	0.07 ± 0.02	0.13 ± 0.03
	60	0.11 ± 0.03	0.13 ± 0.01	0.31 ± 0.02
	120	0.43 ± 0.06	0.31 ± 0.01	0.66 ± 0.05
(−)-*cis*-BPDE				
	10	n.d.	0.31 ± 0.03	0.10 ± 0.01
	30	0.14 ± 0.01	1.58 ± 0.18	0.40 ± 0.02
	60	0.22 ± 0.02	4.44 ± 0.24	1.59 ± 0.09
	120	0.86 ± 0.07	9.88 ± 0.24	5.42 ± 0.73

[a] Primer extension reactions were carried out at 25 °C, using 10 units of exo$^-$ Klenow fragment, as described in the caption to Figure 7. dA, Δ^1, and Δ^2 represent the amount of the fully extended product containing dA, one-base, or two-base deletions opposite the adduct. n.d. means not detectable.

Table II: Sequence Analysis of Extended Primers on BPDE-Modified Templates[a]

	GAGG–5′CCTTCXCTCC–				GAGG–5′CCTTTXCTCC–		
	sequence				sequence		
band	(18′ 13′)		product	band	(18′ 13′)		product
a		G	13G	i		G	13G
b		A	13A	j		A	13A
c		GA	14A or $\Delta^3(-1)$	k		GA	$\Delta^3(-1)$
d		GGA	Δ^3	l		GGA	Δ^3
e		GAA	$\Delta^2(-1)$	m		GAA	$\Delta^2(-1)$
f		GGAA	Δ^2	n		GAAA	$\Delta^1(-1)$
g		GGAAG	Δ^1	o		GAAAA	Δ^1
h		GGAAGA	18A	p		GGAAAA	18A

[a] The sequence of the extended products was established by the Maxam–Gilbert method. Bands a–h in Figure 7 and i–p in Figure 10 were recovered from several experiments; 4000 cpm of each band permits sequence analysis. 18A, 18G, Δ^1, Δ^2, and Δ^3 represent the fully extended product containing dA or dG opposite the lesion and one-, two-, or three-base deletions, respectively. The number indicates the length of the product; for certain deletions, incomplete extension is indicated by a number in parentheses.

the lesion (h, representing 4.65% of the starting primer) and a small amount of 17-mer, representing a one-base deletion (0.16%), were observed. With the dG-(+)-*trans*-BPDE adduct (lane 3), only a small amount of 17-mer containing a one-base deletion (0.37%) was detected. When the dG-(−)-*cis*-BPDE adduct was used (lane 6), a one-base deletion (g, 2.88 %) was produced. The f band (lane 6) represents a two-base deletion (1.25%). With the dG-(+)-*cis*-BPDE adduct (lane 5), a small amount of 18-mer containing dA (0.13%) was detected. 18-mers with dGMP or dTMP incorporated opposite the lesion were not observed (amount of detection, 0.02% of starting primer).

The amount of dAMP misincorporation and/or one- and two-base deletions increased over time, as shown in Figure 8 and Table I. The identity of base substitutions and position of deletions produced by dG-BPDE-modified templates in these experiments was confirmed by Maxam–Gilbert sequence analysis (Maxam & Gilbert, 1980); results are summarized in Table II. A typical analysis, reflecting incorporation of

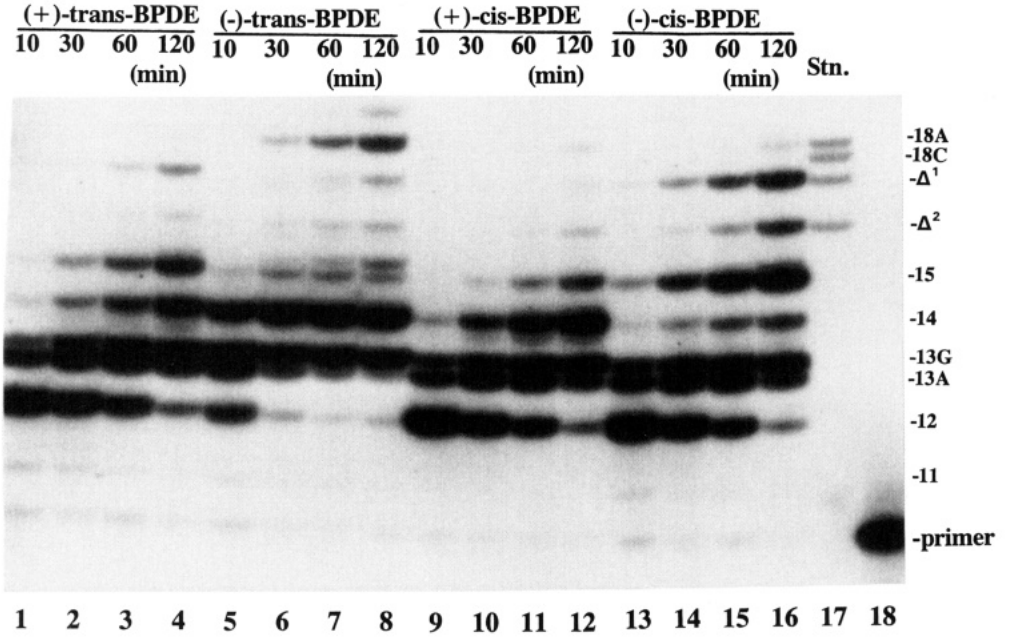

FIGURE 8: Time course of miscoding frequencies on isomeric BPDE modified templates. Primer extension reactions were conducted at 25 °C using 10 units of exo⁻ Klenow fragment as described in the caption to Figure 7.

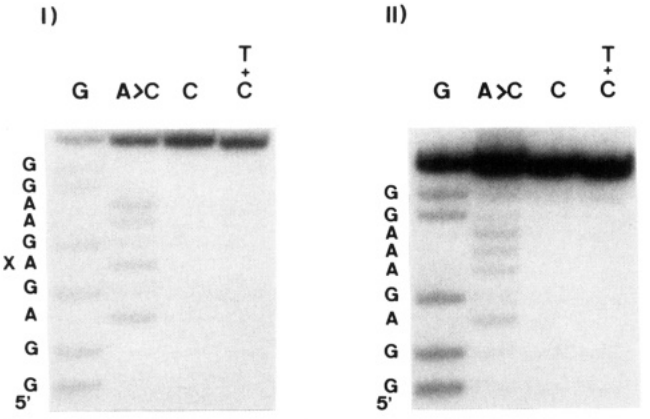

FIGURE 9: Sequence analysis of fully extended primers replicated on DNA templates containing dG-(–)-*trans*-BPDE and dG-(–)-*cis*-BPDE. Fully extended products (18-mers), containing (I) dA opposite dG-(–)-*trans*-BPDE, recovered from lane 4, Figure 7 (5′CCT-TCXCT--), and (II) a one-base deletion opposite dG-(–)-*cis*-BPDE, recovered from lane 6, Figure 10 (5′CCTTTXCT). The nucleotide sequence of these products was established by the Maxam–Gilbert method.

dAMP opposite the dG-(–)-*trans*-BPDE adduct, is shown in Figure 9I). Band c at position 14 in lane 4 (Figure 7) represents a product either four bases shorter than a fully extended product containing dAMP opposite the lesion (14A) or one base shorter than the three-base deletion (Δ^3-1) (A5 and A4 in Figure 11). The two bands observed at position 15 in lane 4 reflect a three-base deletion opposite the lesion (d, upper band) and a product one base shorter than the two-base deletion product (e, lower band) (A4 and A3 in Figure 11).

Extension with exo⁺ Polymerase I. When the exo⁺ Klenow fragment was used for primer extension reactions, extension was blocked opposite and one base before the lesion, although kinetic studies show that dAMP and dGMP are incorporated opposite all dG-BPDE adducts (data not shown). Reaction products were not extended past the lesion. It would appear that the proofreading 3′→5′ exonuclease associated with the Klenow fragment minimizes the amount of base substitutions and deletions.

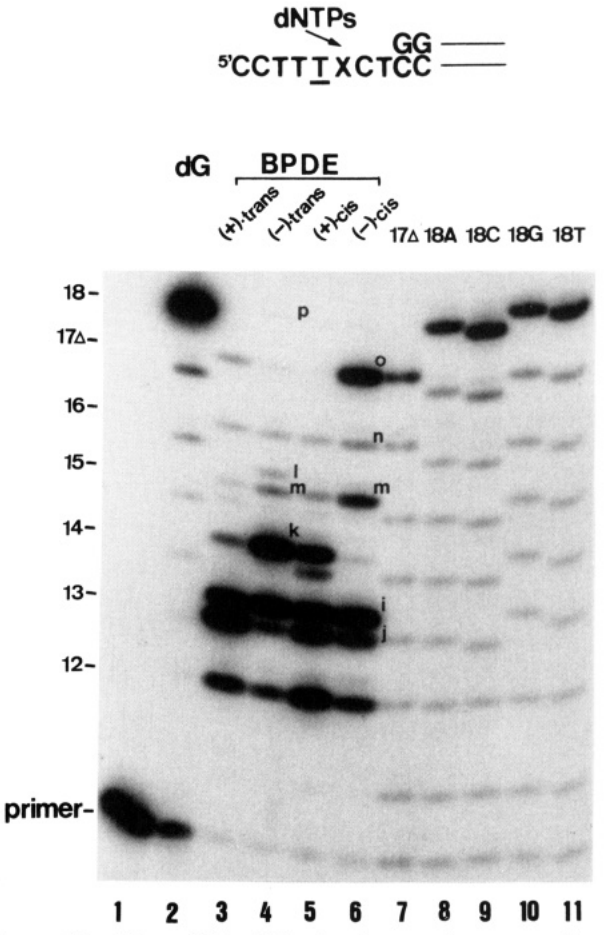

FIGURE 10: Effect of 5′ neighboring base on frequency of base substitution and deletions. 18-mer templates containing dT instead of dC 5′ to the lesions (5′-CCTTTXCTCCTTTCCTCT, X = dG or dG-N2-BPDEs) were used in primer extension reactions as described in the caption to Figure 7. Standards: lanes 7–11, same as those described in the caption to Figure 7.

Kinetic Studies of Nucleotide Insertion and Extension

As shown in Table III, kinetic parameters for base insertion opposite dG-BPDE adducts and extension from the 3′ primer

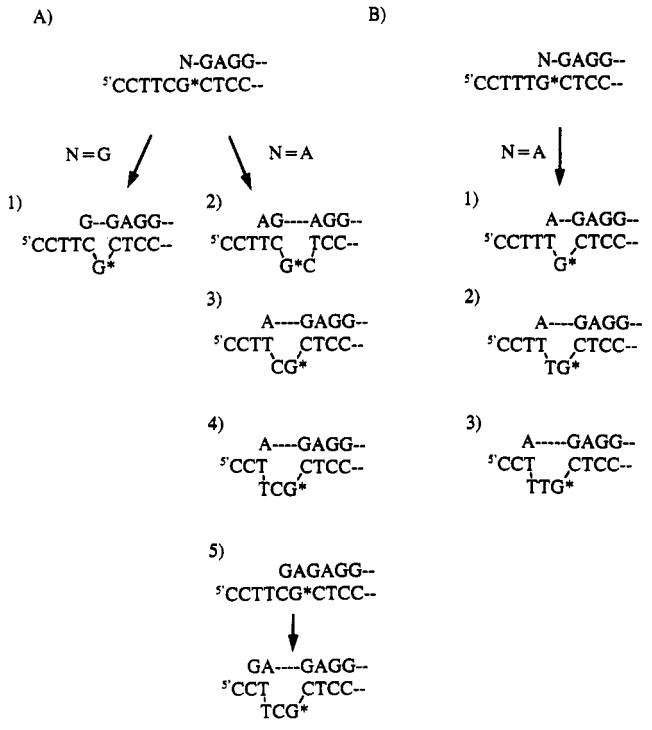

FIGURE 11: Proposed mechanism for one-, two-, and three-base deletions. See text for descriptions of mechanisms A and B and the numbered products.

terminus were determined under steady-state conditions as previously described (Shibutani *et al.*, 1991; Shibutani & Grollman, 1993). For isomeric dG-BPDE adducts, F_{ins} for dNMPs opposite the lesion followed the order: dAMP > dGMP > dTMP > dCMP. F_{ins} for dAMP opposite dG-(−)-*trans*-BPDE was 10 times higher than for dG-(+)-*trans*-BPDE or dG-(−)-*cis*-BPDE and 30 times higher than for dG-(+)-*cis*-BPDE. When chain extension was measured, only the F_{ext} when dA paired with dG-BPDE adducts could be detected. F_{ext} for dA:dG-(−)-*trans*-BPDE pair was 16–150 times higher than for other dA:dG-BPDE pairs. Only the intermediate corresponding to incorporation of dAMP opposite dG-(−)-*trans*-BPDE was extended to form the full-length 18-mer product (Figure 7, lane 4). $F_{ins}F_{ext}$ is used as a parameter to estimate the frequency of lesion bypass (Dosanjh *et al.*, 1991). $F_{ins}F_{ext}$ of dG-(−)-*trans*-BPDE was 280, which is 1500 times higher than that of the other stereoisomeric adducts.

Effect of the 5′ Flanking Base on the Frequency of Base Substitution and Deletion

The frequencies of base substitutions and deletions were determined on templates containing dT 5′ to the dG-BPDE adducts (Figure 10). When a dG-(−)-*cis*-BPDE-modified template was used (lane 6), the frequency of one-base deletions was increased 9.3-fold (25.9%), compared with the sequence containing dC 5′ to the lesion (Figure 7). The identity and position of one-base deletions produced by the dG-(−)-*cis*-BPDE adduct was confirmed by Maxam–Gilbert sequence analysis (Maxam & Gilbert, 1980) (Figure 9). For other dG-BPDE adducts, frequencies of one-base deletions were increased slightly (Figure 10, lanes 3–5). Incorporation of dAMP opposite dG-(−)-*trans*-BPDE decreased from 4.65% to 0.21% (p, lane 4). Thus, the base flanking the lesion on the 5′ side affects relative and overall frequencies of base substitutions and deletions.

Using DNA sequence analysis, the band at the 16 position (n, lane 6) was confirmed as being one base shorter than the product containing a one-base deletion (Table II); its migration is faster than that of the fully extended product containing a

Table III: Kinetic Parameters for Nucleotide Insertion and Chain Extension Reactions Catalyzed by the exo⁻ Klenow Fragment[a]

	dNTP ▼G–^{32}P 12-mer 5′-CCTTCXC–			dGTP ▼NG–^{32}P 13-mer 5′-CCTTCXC–			
N:X	K_M (μM)	V_{max} (% min^{-1})	F_{ins}	K_M (μM)	V_{max} (% min^{-1})	F_{ext}	$F_{ins}F_{ext}$
			X = G				
C:X	2.3 ± 0.9	25.8 ± 0.8	1.0	5.2 ± 0.3	96.1 ± 1.3	1.0	1.0
A:X	67.4 ± 10.7	0.62 ± 0.01	7.46×10^{-4}	19.9 ± 2.0	(7.67 ± 0.49) × 10^{-2}	2.10×10^{-4}	1.57×10^{-7}
G:X	32.2 ± 2.8	1.09 ± 0.02	2.71×10^{-3}	20.6 ± 0.8	4.98 ± 0.04	1.30×10^{-3}	3.52×10^{-6}
T:X	54.4 ± 3.7	1.47 ± 0.01	2.36×10^{-3}	21.0 ± 3.3	20.9 ± 2.1	5.37×10^{-2}	1.27×10^{-4}
			X = G-(+)-*trans*-BPDE				
C:X	91.6 ± 26.2	(1.77 ± 0.54) × 10^{-3}	1.40×10^{-6}	n.d.			
A:X	13.6 ± 2.4	(1.15 ± 0.05) × 10^{-2}	6.82×10^{-5}	77.4 ± 8.7	(2.73 ± 0.23) × 10^{-3}	1.90×10^{-6}	1.30×10^{-10}
G:X	88.2 ± 11.5	(7.39 ± 0.13) × 10^{-3}	6.80×10^{-6}	n.d.			
T:X	115 ± 21	(3.56 ± 1.13) × 10^{-3}	2.60×10^{-6}	n.d.			
			X = G-(−)-*trans*-BPDE				
C:X	90.2 ± 25.2	(3.99 ± 1.58) × 10^{-3}	3.20×10^{-6}	n.d.			
A:X	18.4 ± 2.5	0.16 ± 0.02	6.88×10^{-4}	10.6 ± 1.7	(5.50 ± 0.16) × 10^{-2}	2.81×10^{-4}	1.93×10^{-7}
G:X	23.3 ± 6.7	0.11 ± 0.02	4.16×10^{-4}	n.d.			
T:X	97.8 ± 1.2	(6.74 ± 1.28) × 10^{-3}	5.50×10^{-6}	n.d.			
			X = G-(+)-*cis*-BPDE				
C:X	n.d.			n.d.			
A:X	147 ± 27	(4.25 ± 0.35) × 10^{-2}	2.33×10^{-5}	36.6 ± 1.8	(1.20 ± 0.01) × 10^{-2}	1.76×10^{-5}	4.10×10^{-10}
G:X	159 ± 33	(2.28 ± 0.25) × 10^{-2}	1.16×10^{-5}	n.d.			
T:X	141 ± 22	(8.70 ± 0.59) × 10^{-4}	5.00×10^{-7}	n.d.			
			X = G-(−)-*cis*-BPDE				
C:X	130 ± 24	(2.28 ± 0.11) × 10^{-3}	1.40×10^{-6}	n.d.			
A:X	34.1 ± 4.1	(3.05 ± 0.13) × 10^{-2}	7.19×10^{-5}	19.2 ± 5.5	(3.20 ± 0.84) × 10^{-3}	9.80×10^{-6}	7.03×10^{-10}
G:X	95.7 ± 11.0	(3.62 ± 0.14) × 10^{-2}	3.05×10^{-5}	n.d.			
T:X	51.8 ± 9.7	(2.86 ± 0.04) × 10^{-3}	4.50×10^{-6}	17.2 ± 3.0	(1.10 ± 0.71) × 10^{-3}	3.70×10^{-6}	1.67×10^{-11}

[a] Kinetics of insertion and extension reactions were determined as described under Experimental Procedures. Frequencies of nucleotide insertion (F_{ins}) and chain extension (F_{ext}) were estimated by the equation: $F = (V_{max}/K_M)$[wrong pair]/(V_{max}/K_M)[right pair = dC:dG]. X = unmodified or modified lesion. n.d. = not detectable.

two-base deletion. Band k at position 14 in lane 4 is one base shorter than that of the product of a three-base deletion (Δ^3-1), (B3 in Figure 11). The two bands at position 15 in lane 4 represent a three-base deletion (l, upper band) and a product one base shorter than a two-base deletion (n, lower band) (B2 in Figure 11).

DISCUSSION

Mutagenic Potentials of dG-anti-BPDE Lesions in Vitro. Primer extension reactions catalyzed by DNA polymerase allow us to quantify nucleotide miscoding and deletions in the presence of all four dNTPs and to observe other products formed during translesional synthesis (Shibutani *et al.*, 1991a; Shibutani & Grollman, 1993). We applied this assay to a study of the relative miscoding potential of defined stereoisomeric dG-(+)- and dG-(−)-*anti*-BPDE–oligonucleotide adducts. Misincorporation of dAMP was most prominent on templates containing dG-(−)-*trans-anti*-BPDE (Figure 7). $F_{ins}F_{ext}$, a parameter representing the product of frequency of nucleotide insertion and chain extension, is 2 or 3 orders of magnitude higher for dG-(−)-*trans-anti*-BPDE–oligonucleotide than for the other three stereoisomeric adducts (Table III). Kinetic studies suggest that the exo$^-$ Klenow fragment permits relatively easy bypass of the dG-(−)-*trans*-BPDE lesion. On the other hand, most deletions were produced by the dG-(−)-*cis-anti*-BPDE adduct, the most poorly extended adduct (Table III). Our data indicate that (−)-*anti*-BPDE, which produces dG-(−)-*trans* and dG-(−)-*cis* adducts in native DNA, has greater miscoding potential than (+)-*anti*-BPDE in the *in vitro* system.

Comparisons with in Vivo Mutation Spectra. Mutations induced by racemic (±)-*anti*-BPDE have been investigated in several types of mammalian cells (Yang *et al.*, 1987; Carothers & Grunberger, 1990; Keohavong & Thilly, 1992; Chen *et al.*, 1990, 1991; Mazur & Glickman, 1988) and in bacteria (Bernelot-Moens *et al.*, 1990; Eisenstadt *et al.*, 1982; Mizusawa *et al.*, 1981). These studies include the use of plasmids treated *in vitro* with (±)-*anti*-BPDE (Yang *et al.*, 1987; Roilides *et al.*, 1988; Chakrabarti *et al.*, 1984; Vousden *et al.*, 1986). Mutants analyzed in these studies showed predominantly G→T transversions. The same type of point mutation was dominant when mutations in the *hprt* gene of Chinese hamster embryo cells were induced by the (+)-enantiomer of *anti*-BPDE (Wei *et al.*, 1991). Recent site-directed mutagenesis experiments in which a single dG-(+)-*trans*-BPDE lesion was introduced into an *E. coli* plasmid also showed a preponderance of G→T transversions (Mackay *et al.*, 1992; Rodriguez & Loechler, 1993). In addition, employing racemic *anti*-BPDE, several laboratories have observed a high frequency of one-base deletions (Yang *et al.*, 1987; Bernelot-Moens *et al.*, 1990; Roilides *et al.*, 1988; Chakrabarti *et al.*, 1984; Mizusawa *et al.*, 1981). Thus, results of our *in vitro* studies are qualitatively consistent with mutational spectra observed *in vivo* using either racemic (±)-*anti*-BPDE or (+)-*anti*-BPDE.

It is known that the reaction of (±)-*anti*-BPDE induces several minor adducts, including the labile dG-N7-BPDE adduct, in addition to the major dG-N2-BPDE lesion (Osborne *et al.*, 1978, 1981; King *et al.*, 1979). The dG-N7-BPDE adduct is unstable and depurinates spontaneously to form abasic sites (Osborne *et al.*, 1978; King *et al.*, 1979). dG-N7-BPDE adducts were detected in urine after treating rats with benzo[*a*]pyrene (Autrup & Seremet, 1986). Bernelot-Moens *et al.* (1990) concluded that G→T transversions induced by (±)-*anti*-BPDE proceeded via abasic sites generated by release of the dG-N7-BPDE adduct. Our data indicate that the dG-N2-BPDE adduct *itself* can induce G→T transversions.

When DNA polymerase III*, a replicative enzyme, was used for primer extension assay, DNA synthesis was blocked one base before all BPDE adducts tested (data not shown). In cells, SOS-induction might permit translesional synthesis or could alter mutational patterns, as reported for another bulky adduct, acetylaminofluorene (Burnouf *et al.*, 1989). Thus, a variety of cellular factors in addition to DNA polymerase may be involved in determining mutational specificity in cells.

A Possible Mechanism for Deletion Mutations. One-, two-, and three-base deletions were detected opposite dG-BPDE adducts when 5′-CCTTCG^{BPDE}CTC– was used as a template. We propose a mechanism for this observation based on studies with another bulky adduct, dG-acetylaminofluorene (dG-AAF). Thus, if extension of the dNTP inserted opposite the lesion is blocked, the bases located at the 3′ terminus of the primer may pair with bases 5′ to the lesion on the template, forming a misaligned intermediate that leads to single or multiple deletions (Shibutani & Grollman, 1993). With dG-BPDE adducts, primer extension was partially blocked with incorporation of dAMP and dGMP occurring opposite the lesion. F_{ins} opposite the adduct followed the order: dAMP > dGMP > dTMP > dCMP. In the case of dG-(−)-*cis*-BPDE, dGMP inserted opposite the lesion could pair with dC 5′ to the lesion to form one-base deletions, as shown in A1 in Figure 11. Alternatively, the inserted dAMP and its 5′ flanking dG might pair with TC 5′ to the lesion on the template to form a two-base deletion (A2 in Figure 11). However, when the newly inserted dAMP can pair with dT two bases 5′ to the lesion and extend by two bases (A3 in Figure 11), a fully extended product containing a two-base deletion shortened by one base (e, Figure 7) can be formed. Strong bands were observed at position 14 (c, Figure 7). These bands might be formed when the newly inserted dAMP was extended one base past the lesion and blocked from further extension (Figure 11, A5). If GA at the 3′ terminus of the primer could pair with CT three bases 5′ to the lesion, a three-base deletion would be produced (d, Figure 7). Three-base deletions could also occur when dAMP pairs with dT three bases 5′ to the lesion (Figure 11, A4) and is further extended by one (c, Figure 7) or two bases (d, Figure 7), providing insight into the capability of DNA polymerase to "read" several bases in advance of the base inserted opposite the lesion.

Effect of the 5′ Flanking Base. The flanking base on the 5′ side of the lesion can affect the frequency of deletions. When the flanking base 5′ to dG-(−)-*cis*-BPDE was changed from dC to dT, the frequency of one-base deletions increased 9.3-fold. The nucleotide dAMP, which is inserted more frequently than dGMP opposite the lesion, may facilitate one-base deletions by pairing with dT 5′ to the lesion (B1 in Figure 11). These results are consistent with the general mechanism for frameshift deletions described for dG-AAF (Shibutani & Grollman, 1993).

Bernelot-Moens *et al.* (1990) reported that most one-base deletions involved the loss of G:C base pair within 5′-T(G) sequences containing iterated dG in an *in vivo* experiment using excision–repair-deficient *E. coli*. This observation may indicate that the one-base deletion occurred frequently at 5′-TG^{BPDE} sites, as described in our *in vitro* experiment. For other dG-BPDE adducts, the amount of one-base deletions was increased slightly when the 5′ flanking base was changed from dC to dT. Thus, sequences neighboring the adduct contribute to the overall frequency of deletions observed.

We have also observed two- and three-base deletions, even though dC 5′ to the lesion was replaced by dT. The newly inserted dAMP could pair with dT two bases 5′ to the lesion to form a two-base deletion (m, Figure 10, B2 in Figure 11). When the newly inserted dAMP paired with dT three bases 5′ to the lesion, a one-base shorter (k, Figure 10) or fully extended (l) product containing three-base deletion might be produced (B3 in Figure 11).

Estimates of Mutagenic Potentials of Specific dG-BPDE Lesions in Vivo. It is interesting to compare the results obtained *in vitro* with the mutagenic potential of *anti*-BPDE *in vivo*, even though the polymerases involved are different and DNA repair may substantially alter the *in vivo* results. The relative abundance of the (+)- and (−)-*cis*- and -*trans*-dG-N2-BPDE adducts *in vivo* can be roughly estimated on the basis of differences in reactivities of (+)-*anti*-BPDE and (−)-*anti*-BPDE with respect to covalent adduct formation with native double-stranded DNA. When Chinese hamster V79 cells were treated with either (+)- or (−)-*anti*-BPDE, 94% and 59% of dG-N2-BPDE DNA adducts were formed, respectively (Brookes & Osborne, 1982). In this experiment, 6-fold higher concentrations of (−)-*anti*-BPDE were required to achieve a number of adducts equal to that formed by the reaction of (+)-*anti*-BPDE. Cheng *et al.* (1989) reported that the ratio of dG-(+)-*trans*:dG-(+)-*cis* produced by (+)-*anti*-BPDE *in vitro* was 94:1; the ratio of dG-(−)-*trans*:dG-(−)-*cis* produced by (−)-*anti*-BPDE was 63:22. By applying the analysis directly to calculate the yield of stereoisomers, the ratio of dG-(+)-*trans*:dG-(+)-*cis*:dG-(−)-*trans*:dG-(−)-*cis* would be 36.5:0.39:2.9:1.0. dG-(−)-*trans*-BPDE and dG-(−)-*cis*-BPDE were miscoding lesions in our studies, but their yields in DNA were much lower than that of dG-(+)-*trans*-BPDE. Therefore, dG-(+)-*trans* adducts are expected to dominate the guanine binding spectrum *in vivo*. To a first approximation, and ignoring factors such as differential repair and differences in polymerase specificity *in vivo*, the relative contributions of the different dG-BPDE lesions to the observed mutagenic effects due to racemic BPDE can be thus estimated. The weak miscoding potential of dG-(+)-*trans*-BPDE lesions observed here suggests that their influence may nevertheless be dominant because of the relative abundance of these dG-(+)-*trans*-BPDE adducts in native DNA *in vivo*.

When benzo[*a*]pyrene was metabolized by liver microsomal enzymes obtained from 3-methylcholanthrene-treated rats, (−)-BP 7,8-dihydrodiol was formed in 10-fold excess relative to (+)-BP 7,8-dihydrodiol (Yang & Gelboin, 1976; Thakker *et al.*, 1976, 1977a,b). (−)-BP 7,8-dihydrodiol was further metabolized by the enzyme to (+)-*anti*-BPDE and (−)-*syn*-BPDE in a 6:1 ratio while (+)-BP 7,8-dihydrodiol was converted to (−)-*anti*-BPDE and (+)-*syn*-BPDE in a 1:22 ratio (Thakker *et al.*, 1977a). Microsomes from normal rats were less stereospecific in metabolism of enantiomers of BP 7,8-dihydrodiol. The ratio of (+)-*anti*-BPDE to (−)-*syn*-BPDE was 2:1, and the ratio of (−)-*anti*-BPDE to (−)-*syn*-BPDE was 1:6 (Thakker *et al.*, 1977a). If these observations are combined with the estimated yields produced by (+)-*anti*- or (−)-*anti*-BPDE as shown above, the ratio of (+)-*trans*:(+)-*cis*:(−)-*trans*:(−)-*cis* induced from benzo[*a*]pyrene is 7200:77:2.9:1.0 using the microsomal fraction obtained from 3-methylcholanthrene-treated rats and 1700:18:2.9:1.0 when the microsomal fraction is obtained from untreated rats. Even if dG-(+)-*trans*-BPDE and dG-(+)-*cis*-BPDE had only slight miscoding potential (Table I), the large amount of these lesions generated in DNA might induce significant mutagenicity, as shown in Table IV. The mutation spectra also may be influenced by the different ratios of stereoisomers produced.

Table IV: Comparative Miscoding by BPDE Adducts in DNA[a]

lesion	dA	Δ^1	Δ^2
	Group A		
(+)-*trans*	1370	12000	3530
(+)-*cis*	33	24	51
(−)-*trans*	26	4.1	2.8
(−)-*cis*	0.9	10	5.4
	Group B		
(+)-*trans*	320	2800	830
(+)-*cis*	7.7	5.6	12
(−)-*trans*	26	4.1	2.8
(−)-*cis*	0.9	10	5.4

[a] Miscoding by adducts in DNA was calculated by multiplying the amount of product formed after a 120-min incubation (Table I) by either the estimated ratio of (+)-*trans*:(+)-*cis*:(−)-*trans*:(−)-*cis* adducts (7200:77:2.9:1) obtained using (Group A) the microsomal fraction from 3-methylcholanthrene-treated rats or the ratio of (+)-*trans*:(+)-*cis*:(−)-*trans*:(−)-*cis* adducts (1700:18:2.9:1) obtained using the microsomal fraction from (Group B) untreated rats.

Possible Effects of Adduct Conformations. Adducts derived from covalent binding of (+)- and (−)-*anti*-BPDE to DNA have been classified into two general types: conformers with intercalation characteristics that are prone to carcinogen–base stacking interactions are termed site I, whereas adducts in which the pyrenyl residue is positioned at external, solvent-exposed binding sites are termed site II (Geacintov et al., 1982, 1984; Geacintov, 1988; Harvey & Geacintov, 1988; Gräslund and Jernström, 1989). Both (+)-*trans*-BPDE–and (−)-*trans*-BPDE–oligonucleotide adduct duplexes exhibit site II characteristics, while both *cis*-BPDE adducts exhibit site I characteristics (Geacintov *et al.*, 1991). In (+)-*trans*-BPDE and (−)-*trans*-BPDE, the pyrenyl ring system is situated in the minor groove; in duplexes, the long axis of the pyrenyl ring system is directed toward the 5′ end of the modified strand, while in the (−)-*trans*-BPDE–oligonucleotide duplexes it is tilted more toward the 3′ end (Singh *et al.*, 1991; de los Santos *et al.*, 1992; Cosman *et al.*, 1992). Furthermore, in duplexes containing (+)-*cis*-BPDE lesions, high-resolution NMR methods have also been employed to demonstrate that the pyrenyl ring system is intercalated between adjacent intact base pairs with the deoxyguanosine ring displaced into the minor groove (Cosman *et al.*, 1993); analogous studies with (−)-*cis*-BPDE lesions have not yet been performed. Interestingly, the minor groove site II conformation of the two *trans* adducts appears to be dictated by the presence of the 7- and 8-position OH groups of BPDE, since a BPDE isomer lacking these hydroxyl groups prefers a site I adduct conformation (Geacintov *et al.*, 1982). It is not yet known to what extent these adduct conformations, characteristic of duplexes, are also relevant to partial duplexes undergoing base insertion and extension. With this caveat, some speculative remarks concerning the influence of adduct conformations on our experimental observations will be offered.

It is interesting to note that the frequency of primer extension beyond the adducted G is some 140 times less probable in the case of the (+)-*trans*- than the (−)-*trans*-BPDE–oligonucleotide adduct (Table III). This is consistent with the notion that the pyrenyl residue, which may be oriented toward the 5′ end in the (+)-*trans*-BPDE templates (as it is in the duplexes), inhibits proper base pairing and base–base stacking for base insertion at the 5′ base flanking the modified dG residue on the template strand. In the case of the (−)-*trans*-BPDE adduct, the pyrenyl residue is oriented closer to the 3′ end of the template, thus allowing for proper extension on the 5′ side.

In double-stranded DNA, the aromatic pyrenyl moieties in (+)-*cis*-BPDE (Geacintov *et al.*, 1991; Cosman *et al.*, 1993) and (−)-*cis*-BPDE–dG adducts tend to stack with the neighboring bases. During attempted base insertion opposite the modified guanine, intermediate structures involving misaligned conformations at the adducted sites may form (Figure 11); these "bulges" are more likely to occur in the case of *cis* rather than *trans* adducts, due to stabilization produced by BPDE–base stacking interactions to which *cis* adducts are prone. Thus, the dNMP inserted opposite the lesion might preferentially pair with the base on the 5′ side of the adducted guanine in the template to generate deletions rather than base substitutions (Figure 11).

The dominant insertion of adenine and to a lesser extent guanine opposite the lesions may be due to a preferential formation of intermediate weak complexes between purines and the pyrenyl residues; in contrast to purines, pyrimidines are less prone to form weak noncovalent van der Waals complexes with BPDE derivatives, as has been observed in simple *in vitro* systems (N. E. Geacintov, R. Zhao, V. A. Kuzmin, and L. Pecora, submitted for publication). On the other hand, preferential insertion of dAMP may represent an inherent specificity of DNA polymerases. As discussed above, differences in the dAMP miscoding potentials between (+)-*trans*- and (−)-*trans*-BPDE lesions may be related to the orientation of the pyrene ring systems in these two types of adducts (de los Santos *et al.*, 1992).

NOTE ADDED IN PROOF

Hruszkewycz *et al.* (1992) reported recently that primer extension reactions catalyzed by T7 DNA polymerase (Sequenase 2.0) and human polymerase α are strongly blocked by (+)-*trans*- and (+)-*cis*-BPDE adduct; a small amount of dCMP was preferentially incorporated opposite the lesion. When high concentrations of dNTPs were used, fully extended product(s) were observed. Using Sequenase 2.0 in our experimental system, a small amount of fully extended product containing dCMP was also observed but only opposite (+)-*cis*- or (−)-*cis*-BPDE. The miscoding spectrum generated by Sequenase 2.0 appears to be different from that observed with exo$^-$ Klenow fragment. As reported previously (Shibutani *et al.*, 1991a), the miscoding potential of a given lesion may vary, depending on the DNA polymerase involved in lesion bypass.

ACKNOWLEDGMENT

We thank R. Rieger and I. Kass for preparing the unmodified oligodeoxynucleotides and S. Rigby for typing the manuscript.

REFERENCES

Autrup, H., & Seremet, T. (1986) *Chem.–Biol. Interact. 60*, 217–226.

Basu, A. K., & Essigmann, J. M. (1988) *Chem. Res. Toxicol. 1*, 1–18.

Benasutti, M., Ezzedine, D., & Loechler, E. L. (1988) *Chem. Res. Toxicol. 1*, 160–168.

Bernelot-Moens, C., Glickman, B. W., & Gordon, A. J. (1990) *Carcinogenesis 11*, 781–785.

Brookes, P., & Osborne, M. R. (1982) *Carcinogenesis 3*, 1223–1226.

Brown, W. C., & Romano, L. J. (1991) *Biochemistry 30*, 1342–1350.

Buening, M. K., Wislocki, P. G., Levin, W., Yagi, H., Thakker, D. R., Akagi, H., Koreeda, M., Jerina, D. M., & Conney, A. H. (1978) *Proc. Natl. Acad. Sci. U.S.A. 11*, 5358–5361.

Burgess, J. A., Stevens, C. W., & Fahl, W. E. (1985) *Cancer Res. 45*, 4257–4262.

Burnouf, D., Koehl, P., & Fuchs, R. P. P. (1989) *Proc. Natl. Acad. Sci. U.S.A. 86*, 4147–4151.

Carothers, A. M., & Grunberger, D. (1990) *Carcinogenesis 11*, 189–192.

Chakrabarti, S., Mizusawa, H., & Seidman, M. (1984) *Mutat. Res. 126*, 127–137.

Chen, R.-H., Maher, V. M., & McCormick, J. J. (1990) *Proc. Natl. Acad. Sci. U.S.A. 87*, 8680–8684.

Chen, R-H., Maher V. M., & McCormick, J. J. (1991) *Cancer Res. 51*, 2587–2592.

Cheng, S. C., Hilton, B. D., Roman, J. M., & Dipple, A. (1989) *Chem. Res. Toxicol. 2*, 334–340.

Cosman, M., Ibanez, V., Geacintov, N. E., & Harvey, R. G. (1990) *Carcinogenesis 11*, 1667–1672.

Cosman, M., Santos, C., Fiala, R., Hingerty, B., Singh, S. B., Ibanez, V., Margulis, L. A., Live, D., Geacintov, N. E., Broyde, S., & Patel, D. J. (1992) *Proc. Natl. Acad. Sci. U.S.A. 89*, 1914–1918.

Cosman, M., de los Santos, C., Fiala, R., Hingerty, B. E., Ibanez, V., Luna, E., Harvey, R. G., Geacintov, N. E., Broyde, S., & Patel, D. (1993) *Biochemistry 32*, 4145–4155.

de los Santos, C., Cosman, M., Hingerty, B. E., Ibanez, V., Margulis, L. A., Geacintov, N. E., Broyde, S., & Patel, D. J. (1992) *Biochemistry 31*, 5245–5252.

Dosanjh, M. K., Galeros, G., Goodman, M. F., & Singer, B. (1991) *Biochemistry 30*, 11595–11599.

Eisenstadt, E., Warren, J., Porter, J., Atkins, D., & Miller, J. H. (1982) *Proc. Natl. Acad. Sci. U.S.A. 79*, 1945–1949.

Geacintov, N. E. (1988) in *Polycyclic Aromatic Hydrocarbon Carcinogenesis: Structure-Activity Relationships* (Yang, S. K., & Silverman, B. D., Eds.) Vol. II, pp 181–206, CRC Press, Boca Raton, FL.

Geacintov, N. E., Gagliano, A. G., Ibanez, V., & Harvey, R. G. (1982) *Carcinogenesis 3*, 247–253.

Geacintov, N. E., Yoshida, H., Ibanez, V., Jacobs, S. A., & Harvey, R. G. (1984) *Biochem. Biophys. Res. Commun. 122*, 33–39.

Geacintov, N. E., Cosman, M., Mao, B., Alfano, A., Ibanez, V., & Harvey, R. G. (1991) *Carcinogenesis 12*, 2099–2108.

Gräslund, A., & Jernström, B. (1989) *Q. Rev. Biophys. 22*, 1–37.

Harvey, R. G., & Geacintov, N. E. (1988) *Acc. Chem. Res. 21*, 66–73.

Hruszkewycz, A. M., & Dipple, A. (1991) *Carcinogenesis 12*, 2185–2187.

Hruszkewycz, A. M., Canella, K. A., & Dipple, A. (1991) *Carcinogenesis 12*, 1659–1663.

Hruszkewycz, A. M., Canella, K. A., Peltonen, K., Kotrappa, L. & Dipple, A. (1992) *Carcinogenesis 13*, 2347–2352.

Hsu, I. C., Bowden, G. T., & Harris, C. C. (1979) *Mutat. Res. 63*, 351–359.

Huberman, E., Sachs, L., Yang, S. K., & Gelboin, H. V. (1976) *Proc. Natl. Acad. Sci. U.S.A. 73*, 607–611.

Jeffrey, A. M., Jennette, K. W., Blobstein, S. H., Weinstein, I. B., Beland, F. A., Harvey, R. G., Kasai, H., Miura, I., & Nakanishi, K. (1976) *J. Am. Chem. Soc. 98*, 5714–5715.

Jeffrey, A. M., Grzeskowiak, K., Weinstein, I. B., Nakanishi, K., Roller, P., & Harvey, R. G. (1979) *Science 206*, 1309–1311.

Kapitulnik, J., Wislocki, P. G., Levin, W., Yagi, H., Thakker, D. R., Akagi, H., Koreeda, M., Jerina, M., & Conney, A. H. (1978). *Cancer Res. 38*, 2661–2665.

Keohavong, P., & Thilly, W. G. (1992) *Proc. Natl. Acad. Sci. U.S.A. 89*, 4623–4627.

King, H. W. S., Osborne, M. R., & Brookes, P. (1979) *Chem.–Biol. Interact. 24*, 345–353.

Koreeda, M., Moore, P. D., Wislocki, P. G., Levin, W., Conney, A. H., Yagi, H., & Jerina, D. M. (1978) *Science 199*, 778–781.

Larson, K. L., & Strauss, B. S. (1987) *Biochemistry 26*, 2471–2479.

Mackay, W., Benasutti, M., Droulin, E., & Loechler, E. L. (1992) *Carcinogenesis 13*, 1415–1425.

Malavelle, C., Kuroki, T., Sims, P., Grover, P. L., & Bartsch, H. (1977) *Mutat. Res. 44*, 313–326.
Maxam, A. M., & Gilbert, W. (1980) *Methods Enzymol. 65*, 499–560.
Mazur, M., & Glickman, B. W. (1988) *Somat. Cell Mol. Genet. 14*, 393–400.
Meehan, T., & Straub, K. (1979) *Nature 277*, 410–412.
Mendelman, L. V., Boosalis, M. S., Petruska, J., & Goodman, M. F. (1989) *J. Biol. Chem. 264*, 14415–14423.
Mendelman, L. V., Petruska, J., & Goodman, M. F. (1990) *J. Biol. Chem. 265*, 2338–2346.
Mizusawa, H., Lee, C-H., Kakefuda, T., McKenney, K., Shimatake, H., & Rosenberg, M. (1981) *Proc. Natl. Acad. Sci. U.S.A. 78*, 6817–6820.
Newbold, R. F., & Brookes, P. (1976) *Nature 261*, 52–54.
Newbold, R. F., Brookes, P., & Harvey, R. G. (1979) *Int. J. Cancer 24*, 203–209.
Osborne, M. R., Harvey, R. G., & Brookes, P. (1978) *Chem.–Biol. Interact. 20*, 123–130.
Osborne, M. R., Jacobs, S., Harvey, R. G., & Brookes, P. (1981) *Carcinogenesis 2*, 553–558.
Reardon, D. B., Bigger, C. A. H., & Dipple, A. (1990) *Carcinogenesis 11*, 165–168.
Rodriguez, H., & Loechler, E. L. (1993) *Carcinogenesis 14*, 373–383.
Roilides, E., Gielen, J. E., Tuteja, N., Levine, A. S., & Dixon, K. (1988) *Mutat. Res. 198*, 199–206.
Sayer, J. M., Chadha, A., Agarwal, S. K., Yeh, H. J. C., Yagi, H., & Jerina, D. M. (1991) *J. Org. Chem. 56*, 20–29.
Shibutani, S., & Grollman, A. P. (1993) *J. Biol. Chem. 268*, 11703–11710.
Shibutani, S., Takeshita, M., & Grollman, A. P. (1991a) *Nature 349*, 431–434.
Shibutani, S., Gentles, R., Johnson, F., & Grollman, A. P. (1991b) *Carcinogenesis 12*, 813–818.
Singer, B., & Essigman, J. M. (1991) *Carcinogenesis 12*, 949–955.
Singh, S. B., Hingerty, B. E., Singh, U. C., Greenberg, J. P., Geacintov, N. E., & Broyde, S. (1991) *Cancer Res. 51*, 3482–3492.
Slaga, T. J., Bracken, W. J., Gleason, G., Levin, W., Yagi, H., Jerina, D. M., & Conney, A. H. (1979) *Cancer Res. 394*, 67–71.
Stevens, C. W., Bouck, N., Burgess, J. A., & Fahl, W. E. (1985) *Mutat. Res. 152*, 5–14.
Strauss, B. S. (1991) *BioEssays 13*, 79–84.
Takeshita, M., Chang, C.-N., Johnson, F., Will, S., & Grollman, A. P. (1987) *J. Biol. Chem. 262*, 10171–10179.
Thakker, D. R., Yagi, H., Lu, A. Y. H., Levin, W., Conney, A. H., & Jerina, D. M. (1976) *Proc. Natl. Acad. Sci. U.S.A. 73*, 3381–3385.
Thakker, D. R., Yagi, H., Akagi, H., Koreeda, M., Lu, A. Y. H., Levin, W., Wood, A. W., Conney, A. H., & Jerina, D. M. (1977a) *Chem.–Biol. Interact. 16*, 281–300.
Thakker, D. R., Yagi, H., Levin, W., Lu, A. Y. H., Conney, A. H., & Jerina, D. M. (1977b) *J. Biol. Chem. 252*, 6328–6334.
Thrall, B. D., Mann, D. B., Smerdon, M. J., & Springer, D. L. (1992) *Carcinogenesis 13*, 1529–1534.
Vousden, K. H., Bos, J. L., Marshall, C. J., & Phillips, D. H. (1986) *Proc. Natl. Acad. Sci. U.S.A. 83*, 1222–1226.
Weems, H. B., & Yang, S. K. (1989) *Chirality 1*, 276–283.
Wei, S. J. C., Chang, R. L., Wong, C.-Q., Bhachech, N., Cui, X. X., Hennig, E., Yagi, H., Sayer, J. M., Jerina, D. M., Preston, B. D., & Conney, A. H. (1991) *Proc. Natl. Acad. Sci. U.S.A. 88*, 11227–11230.
Weinstein, I. B., Jeffrey, A. M., Jennette, K. W., Blobstein, S. H., Harvey, R. G., Harris, C., Autrup, H., Kasai, H., & Nakanishi, K. (1976) *Science 193*, 592–594.
Wood, A. W., Chang, R. L., Levin, W., Yagi, H., Thakker, D. R., Jerina, D. M., & Conney, A. H. (1977) *Biochem. Biophys. Res. Commun. 77*, 1389–1396.
Yang, J-L., Maher, V. M., & McCormick. J. J. (1987) *Proc. Natl. Acad. Sci. U.S.A. 84*, 3787–3791.
Yang, J-L., Chen, R-H., Maher, V. M., & McCormick, J. J. (1991) *Carcinogenesis 12*, 71–75.
Yang, S. K., & Gelboin, H. V. (1976) *Biochem. Pharmacol. 25*, 2221–2225.
Yang, S. K., McCourt, D. W. Roller, P. P., & Gelboin, H. V. (1976) *Proc. Natl. Acad. Sci. U.S.A. 73*, 2594–2598.